Optical trapping of an ion

Ch. Schneider, M. Enderlein, T. Huber and T. Schaetz*

Isolating ions and atoms from the environment is essential in experiments on a quantum level[1-4]. For decades, this has been achieved by trapping ions with radiofrequency[5] fields and neutral particles with optical fields[6]. Here we demonstrate the trapping of an ion by interaction with light. The lifetime in the optical trap is several milliseconds, allowing hundreds of oscillations in the optical potential, and could be enhanced by established methods[6]. These results could form the starting point for combining the advantages of optical trapping and ions. Extending the approach to optical lattices could support developments in experimental quantum simulations[7]. As well as simulating complex spin systems with trapped ions, a new class of quantum simulations could be enabled that combines atoms and ions in a common lattice (Cirac, J.I., personal communication; Zoller, P., personal communication). Furthermore, ions could be embedded into quantum degenerate gases, thereby avoiding the inevitable excess kinetic energy of ions in radiofrequency traps, which currently limits cold-chemistry experiments[8,9].

Quantum spin models are a paradigm for the study of intriguing many-body effects such as quantum phase transitions[7], but many problems remain unresolved due to their complexity. It has been shown that a broad class of quantum spin models can be simulated with trapped ions[10,11]. Two electronic levels of the ion can simulate the spin states, and readily controllable light fields induce state-dependent a.c. Stark shifts. The related forces allow the simulation of a state-dependent interaction between the spins. A major advantage of an array of ions over atoms in an optical lattice is that the effective spin–spin interaction is mediated by the Coulomb force. It is therefore orders of magnitude larger than that between atoms in neighbouring sites of the lattice. However, quantum simulation (QS) experiments based on several ions within one radiofrequency (RF) potential are difficult to scale[7]. One option for achieving scalability might be to reduce the distances between ions in arrays of individual RF traps[12], but this has not been achieved to date. An alternative approach is to use ions in an optical lattice that have a related interaction strength sufficiently larger than the relevant decoherence rates (see Methods for specific values). This is similar to a proposal in ref. 13 regarding polar molecules, a topic that is presently attracting considerable experimental effort[14,15].

New classes of QS might become feasible by combining optically trapped ions and atoms in common optical lattices. It is proposed that atoms and ions share charges via tunnelling electrons, leading to intriguing collective states and new ways of simulating the Bose–Hubbard Hamiltonian (Cirac, J.I., personal communication; Zoller, P., personal communication). The ion(s) could either be transferred from a RF trap into the optical lattice filled with atoms, or could be created by photo-ionization of atoms *in situ*.

Optically trapped ions may also be used to overcome severe technical limitations of RF traps. In particular, the comfortable potential depth of RF traps comes at the price of RF-driven micromotion[16]. Overlapping ions in RF traps with atoms in optical traps leads to a RF-induced heating, which currently limits the minimal

collision energy to the order of millikelvins in cold collision experiments[8,9]. One could use a Bose–Einstein condensate of atoms at a temperature of 200 nK as a bath for sympathetic cooling as in ref. 9, but trapping the ion optically. Hence, the range of collision energies below microkelvins and the regime of ultracold chemistry might be entered, where quantum phenomena are predicted to dominate[4].

These promising approaches have not been considered in the past because of the coupling of ions to the static and RF electric fields being stronger than the much weaker coupling of atoms and ions to optical fields. On the one hand, this allowed RF and static electromagnetic ion traps (depths of $\sim 10^4$ K) decades before traps for neutral atoms[5,6] (see Supplementary Information). On the other hand, the Coulomb force leads to a high sensitivity to stray electric fields, which accounts for the supposition that ions would not be trappable in comparatively weak optical potentials (depths of dipole traps $\sim 10^{-3}$ K). However, dipole forces have been used on ions in RF traps to achieve several aims, including ground-state cooling, quantum logic gates and entanglement preparation[17].

In this Letter we describe the first implementation of an optical dipole trap for ions. We demonstrate that optical trapping of ions is feasible, even in proximity to electrodes and dielectrics. The lifetime in the optical potential is currently limited by heating due to photon recoils out of the optical field and, therefore, could be enhanced by established techniques.

The experimental sequence is illustrated in Fig. 1. Initially, the ion is loaded and cooled in a RF trap (Fig. 1a). Subsequently, the RF potential is ramped down to zero and substituted by the dipole trap (Fig. 1b). Finally, the RF potential is ramped up again and the ion can be detected. To be more specific, a single $^{24}\text{Mg}^+$ ion is created by photo-ionization from a thermal atomic beam and is Doppler cooled to a few millikelvins (Doppler cooling limit, 1 mK) in the segmented linear RF trap[18]. The radial frequencies of the RF trap arise from the RF potential and are set to $\omega_{x,y} \approx 2\pi \times 900$ kHz. The axial frequency is tuned to $\omega_z \approx 2\pi \times 45$ kHz by applying appropriate d.c. voltages to the outer d.c. electrodes (Fig. 1). The d.c. field is retained during the entire experiment to prevent the ion from leaving the dipole trap along the propagation direction of the dipole trap beam.

In the next step, stray electric fields are minimized at the position of the ion to reduce their resulting forces to a level smaller than the maximal force of the dipole trap. The voltage applied to an inner d.c. electrode is fine-tuned on the order of few 100 µV, corresponding to a residual force on the order of 10^{-20} N at the position of the ion.

Ramping down the RF voltage during the transfer of the ion from the RF trap to the dipole trap also requires a careful choice of the d.c. voltages to minimize the impact of the unavoidable violation of the stability criteria of the RF trap (for a stability diagram, see ref. 5). Additionally, the RF voltage is ramped down within 50 µs, which is considered fast enough to avoid excessive heating due to higher-order resonances[19]. However, it is slow compared to the oscillation period of the ion and minimizes heating due to a non-adiabatic transfer.

Max-Planck-Institut für Quantenoptik, Hans-Kopfermann-Straße 1, 85748 Garching, Germany. *e-mail: tobias.schaetz@mpq.mpg.de
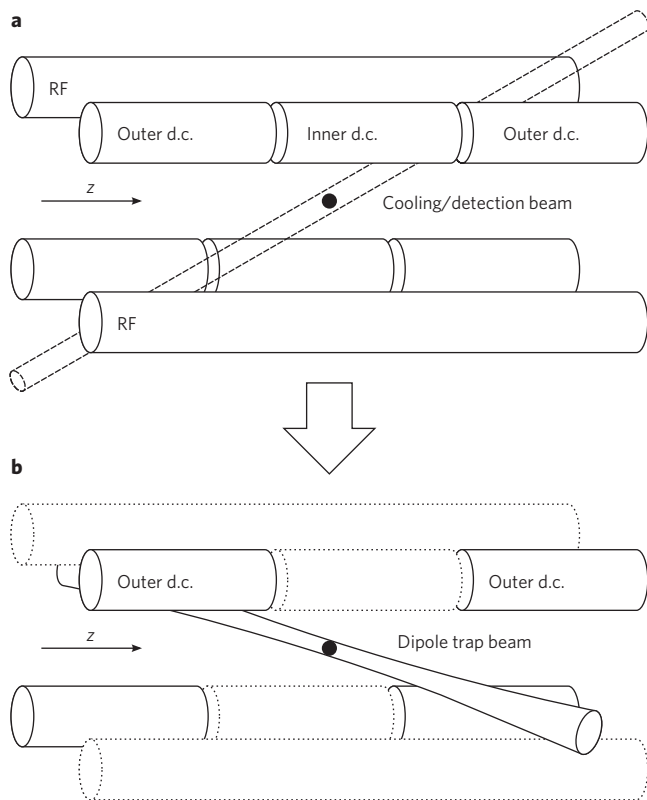
Figure 1 | Two alternative trapping setups. a, Preparation of the ion while trapping with the segmented linear RF trap and cooling with the Doppler laser. The RF electrodes provide the radial confinement, and voltages on the outer d.c. electrodes prevent the ion from escaping axially. The arrow labelled 'z' indicates the axis of the RF trap. **b**, Trapping the ion with the dipole trap laser, which crosses the z-axis at an angle of 45°. The RF potential of the RF trap and the Doppler cooling lasers are turned off, while d.c. fields prevent the ion from leaving the dipole trap along the propagation direction of the beam.

The dipole trap laser[20] at a wavelength of $\lambda = 280$ nm typically provides a power of $P_{optical} = 190$ mW in the dipole trap beam. It is detuned by approximately $\Delta = -2\pi \times 275$ GHz red of the resonance of the $S_{1/2} \leftrightarrow P_{3/2}$ transition of ^{24}Mg$^+$, with a natural line width of $\Gamma = 2\pi \times 41.8$ MHz and a transition frequency of $\omega_0 \approx 2\pi c/280$ nm. The beam is focused on the ion and has a nearly Gaussian shape with a waist radius of $w_0 \approx 7$ μm ($1/e^2$ radius of intensity). The polarization is tuned to σ^+. According to these parameters we expect a depth of the dipole potential[21] of $U_0 = (3c^2/\omega_0^3)(\Gamma/\Delta)(P_{optical}/w_0^2) \approx -k_B \times 38$ mK, where k_B is the Boltzmann constant, and a maximum force perpendicular to the beam of $F_{rad} \approx 1 \times 10^{-19}$ N. The corresponding trapping frequencies at the approximately harmonic bottom of the dipole potential are $\omega_{rad} \approx 2\pi \times 165$ kHz perpendicular to and $\omega_k \approx 2\pi \times 2$ kHz in the direction of beam propagation. The depth of the total potential, consisting of the dipole potential superimposed by the static electric potential, is discussed later.

The transfer into the dipole trap consists of the following steps. (1) The Doppler cooling laser is switched off, (2), the dipole trap laser is then switched on, and (3), the RF potential is ramped down to zero. The dipole trap is kept on for the dipole trap duration $T_{optical}$. Subsequently, the sequence is reversed for the transfer back into the RF potential. A charge coupled device camera is used to monitor the fluorescence light scattered off the ion from the Doppler cooling laser. This reveals with near unity efficiency whether the ion was lost during the experimental sequence. Trapping according to the above sequence is repeated until the ion is lost.

To obtain the lifetime of the ions in the dipole trap we measured the optical trapping probability P. This is determined as the mean number of successful trapping attempts with approximately 40 ions (for example, corresponding to more than 200 attempts for $T_{optical} = 1$ ms in Fig. 2).

Figure 2 shows the optical trapping probability P as a function of the dipole trap duration $T_{optical}$ for a beam power of $P_{optical} = 190$ mW. The near unity probability for dipole trap durations below 1 ms drops to ~20% for 4 ms. The half-life $T_{optical}^{(1/2)} \approx 2.4$ ms of ions in the dipole trap is derived from the dashed curve based on the model introduced below.

Figure 3 presents the optical trapping probability P as a function of the beam power $P_{optical}$ at $T_{optical} = 0.5$ ms. Again, the optical trapping probability approaches unity for high laser powers, which correspond to deep traps. Shallower traps lead to reduced trapping probabilities, and for $P_{optical} = 0$ mW, ions are lost without exception. This emphasizes that other than the dipole trap there is no relevant residual trapping potential during $T_{optical}$.

The dashed curves in Figs 2 and 3 are based on a simple truncated Boltzmann model (see also ref. 22). The particle energies E are assumed to be subject to the Boltzmann distribution of a three-dimensional harmonic potential: $f(E) \propto E^2 \exp(-E/k_B T)$. The temperature is assumed to increase linearly in time t with the heating rate R from an initial value T_0: $T = (T_0 + Rt)$. Both the potential depth $|U_0|$ and the heating rate R are assumed to be proportional to $P_{optical}$. The optical trapping probability is obtained as the probability for an ion to have an energy $E \leq |U_0|$ at $T_{optical}$. The relevant experimental parameters differ by less than 10% between Figs 2 and 3. A joint fit yields parameters $T_0 = 4.6$ mK and $R = 3.9$ mK ms$^{-1} \times P_{optical}/(190$ mW$)$. The uncertainty of the waist of ± 1 μm relates to an error of 30%.

It has to be considered that the depth of the total trap potential is smaller than $|U_0|$ due to the defocusing effects of the static electric potential. A reduction of the potential depth assumed in the simple model would only decrease the values of T_0 and R, but leave the shapes of the fitted curves in Figs 2 and 3 unchanged. However, as the potential can (temporarily) trap particles with energy up to
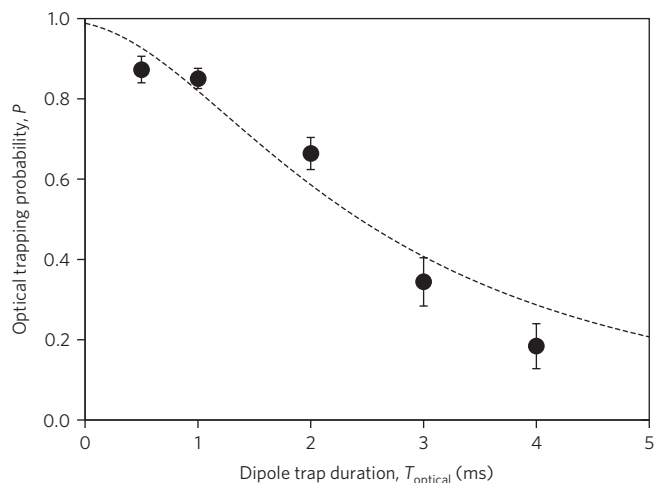

Figure 2 | Optical trapping probability P as a function of dipole trap duration $T_{optical}$. Optical trapping probability is determined as the mean number of successful trapping attempts. Each data point represents experiments on typically 40 ions until each one is lost. Error bars represent standard deviation of the mean. The fitted curve (dashed line) is based on a truncated Boltzmann model (see text). Experimental parameters (errors smaller than 5% unless noted otherwise): beam waist radius $w_0 = (7\pm1)$ μm, laser detuning $\Delta = -2\pi \times 275$ GHz, power of the dipole trap beam $P_{optical} = 190$ mW, axial d.c. frequency $\omega_z = 2\pi \times 47$ kHz, RF off.
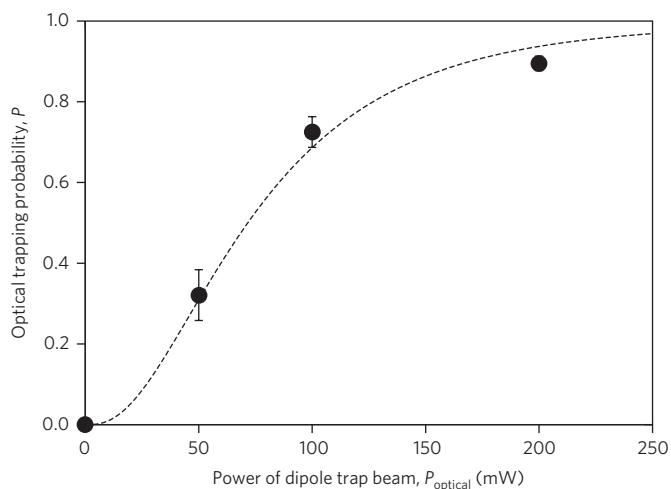
Figure 3 | Optical trapping probability P as a function of power $P_{optical}$ of the dipole trap beam. Probability is determined as for Fig. 2. Error bars represent the standard deviation of the mean, and the fitted curve (dashed line) is based on the same truncated Boltzmann model with identical values for the fit parameters (see text). Experimental parameters (errors smaller than 5% unless noted otherwise): beam waist radius $w_0 = (6.5 \pm 1.0)$ μm, laser detuning $\Delta = -2\pi \times 300$ GHz, dipole trap duration $T_{optical} = 0.5$ ms, axial d.c. frequency $\omega_z = 2\pi \times 41$ kHz, RF off.

approximately $2|U_0|$ due to angular momentum considerations, and the potential is not decreased in all directions by the defocusing effects, $|U_0|$ is still a good estimate for the 'effective' potential depth in the simple model.

The experimental parameters (Fig. 2) lead to a maximal scattering rate[21] of $\Gamma_{s,max} = (U_0/\hbar)(\Gamma/\Delta) \approx 750$ ms^{-1} in the centre of the dipole trap. A single scattering event leads to the transfer of a mean energy $2E_r \approx k_B \times 10$ μK. This corresponds to a maximal recoil heating rate of $R_{s,max} = 2E_r \times \Gamma_{s,max} = 7.5$ mK ms^{-1}. The heating rate R obtained from the fit is a factor of two smaller than $R_{s,max}$. This can be explained by the reasonable assumption of a time-averaged heating rate $\bar{R}_s \approx R_{s,max}/2$ due to the spatial dependence of the scattering rate Γ_s experienced by the oscillating ion in the dipole potential. A plausible estimate of the 'maximal' duration after which an ion with zero initial temperature will be lost can be given by the ratio $|U_0|/(R_{s,max}/2)$. This is equal to 10 ms and agrees with our observations. We therefore conclude that heating is mainly caused by photon scattering and not by fluctuating residual electric fields. This also justifies the assumption $R \propto P_{optical}$ in our model. The result is in agreement with theoretical examinations of heating effects in dipole traps[23], yielding recoil heating as the main source for our experimental parameters and negligible heating due to dipole force fluctuations (<0.01 mK ms^{-1}), for example.

The initial temperature T_0 derived from our model is comparable to the estimated temperature of the Doppler cooled ion in the RF trap before transfer. This suggests that loading into the dipole potential is performed with little heating. However, the experimental trapping probability reaches a maximum of $P \approx 0.9$. Trapping attempts with a duration $T_{optical} \ll 0.5$ ms did not significantly exceed this value either. According to our model, the non-zero initial temperature T_0 only accounts for a 1% effect (see Fig. 2). We assume two reasons for the reduced P in the experiment. First, the minimum of the dipole potential might not always sufficiently overlap with the position of the ion at turn-off of the RF trap due to beam pointing instabilities. Also, insufficient minimization of residual static electric fields can give rise to ion loss even at zero $T_{optical}$.

Our experimental set-up leaves room for substantial technical improvements. The main technical challenges are (1) to achieve a

long lifetime and (2) to incur sufficiently small motional heating and electronic decoherence rates. These points can be addressed by increasing the detuning Δ to reduce the currently limiting scattering rate Γ_s. The commercially available laser system in ref. 24 can provide more than 40 W at a wavelength of 1,120 nm (Toptica Photonics AG, personal communication). It could approximately reproduce the current trapping conditions, but reduced the scattering rate to the order of 0.07 ms^{-1} (see Methods). Furthermore, the influence of electric potentials can be mitigated by increasing the electrode–ion distance (currently only $R_0 = 0.8$ mm). Depending on the application, an initialization of the ion in the motional ground state[16] before transfer into the optical potential might be sufficient. Otherwise, conventional cooling (Doppler, sideband, Sisyphos cooling) should further enhance the lifetime and cavity cooling, as demonstrated in ref. 25, might not even have to affect the electronic coherence.

For the envisioned QS based on interaction between ions, a sufficiently large strength J of the effective spin–spin interaction has also to be provided. Because optical trapping and simulation of the interaction between the ions are both accomplished by means of a.c. Stark shifts of the electronic levels, we propose disentangling their function through the use of two separate, but commensurate optical lattices. Trapping could be realized by the laser at 1,120 nm, fulfilling the required trapping conditions and providing small mutual distances between the ions. It would cause the same shift to all electronic ground and excited states, respectively, because its detuning is large compared to the fine-structure splitting ($\omega_{P_{1/2} \leftrightarrow P_{3/2}} \approx 2\pi \times 2.7$ THz for Mg). The spin–spin interaction could be simulated by our current laser system at 280 nm at low intensity with detuning providing the required state-dependent shift of the electronic levels[11]. The envisioned interaction strength between ions could be on the order of $J > h$ kHz and, therefore, sufficiently larger than the decoherence rates (see Methods).

Our experimental results open up a variety of further prospects. Novel applications have been proposed for hybrid set-ups, combining optical and RF trap potentials. For example, superimposing a commensurate optical lattice on an ordered structure of ions should allow for QS experiments of mesoscopic two- or even three-dimensional quantum systems[26,27], with the ions either trapped within an array of RF traps individually or forming a Coulomb crystal frozen within a single RF trap. Having optical potentials available that are sufficient for independent trapping allows the design of new set-ups. For example, the RF field could provide radial confinement, and an optical standing wave along the axis could realize the axial confinement, allowing the mutual ion distances to be set. Choosing blue-detuned light would position the ions in the 'dark' lattice sites, reducing Γ_s and thereby allowing for much smaller mutual ion distances and larger interaction strengths J.

Furthermore, it might be advantageous to take advantage of the charge of trapped particles in a variety of proposed applications, but avoid RF-driven micromotion by using purely optical traps. It could avoid limitations where ions are suggested as the ultimate 'objective' of a microscope[28] or 'read/write head'[26] in conventional traps.

In summary, we have achieved optical trapping of an ion, even in close proximity to electrodes. We have also shown that hybrid set-ups, combining optical and RF potentials, are capable of covering the full range of confinements, from RF to optical. The lifetime of the ion in the optical dipole trap is limited by photon scattering, and is therefore expected to be improvable by established techniques. We see our results as the starting point of experiments that merge the fields of trapped atoms and ions, allowing the circumvention of the intrinsic constraints of current proposals and opening new perspectives for QS based on trapped ions and atoms in optical lattices.

Methods

Towards scalability of quantum simulations. For simplicity, we have assumed the one-dimensional confinement of Mg ions in a standing wave along the laser beams only. The set-up could be extended to provide strong confinement in more dimensions by using additional beams (or other configurations, such as cavities or microlens arrays, and other atomic species).

Retro-reflecting the dipole trap beam in the current set-up would provide a boost of the maximal optical force in the direction of the laser beam to 5×10^{-17} N. This force is of the same order of magnitude as the repulsion of two ions at a mutual distance of $d_{min} = 2\,\mu m$. The depth of the total potential of the standing wave and an adjacent ion at a distance of $d = 3\,\mu m$ would still amount to $k_B \times 40$ mK. However, QS would be severely limited by the large decoherence rates due to scattering, for example.

As a slight modification of the present set-up, a commercial laser system (Toptica Photonics AG, personal communication) could provide a beam power of $P'_{optical} = 37.5$ W $\approx 197 \times P_{optical}$ and a wavelength of 1,120 nm, corresponding to a detuning of $\Delta' = 2\pi \times 803$ THz $\approx 2,920 \times \Delta$, that could address this issue and achieve a state-independent optical lattice for trapping. The potential depth within a standing wave formed by beams with waist radii of $w_0 = 7\,\mu m$ can be derived as $U'_0 \approx U_0/4 \approx -k_B \times 10$ mK. At the same time, the maximal photon scattering rate within the standing wave decreases by to $\Gamma'_s \approx 0.07$ m^{-1}. For this configuration we obtain $d_{min} = 17\,\mu m$ and for a distance $d = 19\,\mu m$ to the adjacent ion, a depth of the total potential of $\sim k_B \times 1$ mK.

The oscillation frequency would amount to $\omega_k \approx 2\pi \times 2.4$ MHz. The strength of the effective spin–spin interaction simulated by our currently used laser system at 280 nm can be estimated using the relation[10] $J \propto 1/(\omega_k^4 d^3)$. With the values from our former experiment[11], $J \approx h \times 22$ kHz, $\omega_k = 2\pi \times 3.63$ MHz and $d \approx 4\,\mu m$, we obtain an interaction strength of $J > h$ kHz. Hence, the interaction strength could be sufficiently larger than the decoherence rates through, for example, spontaneous emission (0.07 ms^{-1}), (in)elastic collisions with residual gas[16] (<0.004 s^{-1} (0.03 s^{-1})), motional heating in RF traps[16] (0.02 quanta ms^{-1}), and intensity and frequency noise of the laser[29] (Toptica Photonics AG, personal communication) (0.075 quanta ms^{-1}). A cryogenic environment might also be advantageous, depending on the experimental requirements.

References

1. Nielsen, M. A. & Chuang, I. L. *Quantum Computation and Quantum Information*, Cambridge Series on Information and the Natural Sciences (Cambridge Univ. Press, 2000).
2. Rosenband, T. *et al.* Frequency ratio of Al$^+$ and Hg$^+$ single-ion optical clocks; metrology at the 17th decimal place. *Science* **319,** 1808–1812 (2008).
3. Ye, J., Kimble, H. J. & Katori, H. Quantum state engineering and precision metrology using state-insensitive light traps. *Science* **320,** 1734–1738 (2008).
4. Weiner, J., Bagnato, V. S., Zilio, S. & Julienne, P. S. Experiments and theory in cold and ultracold collisions. *Rev. Mod. Phys.* **71,** 1–85 (1999).
5. Paul, W. Electromagnetic traps for charged and neutral particles. *Rev. Mod. Phys.* **62,** 531–540 (1990).
6. Phillips, W. D. Nobel lecture: laser cooling and trapping of neutral atoms. *Rev. Mod. Phys.* **70,** 721–741 (1998).
7. Buluta, I. & Nori, F. Quantum simulators. *Science* **326,** 108–111 (2009).
8. Grier, A. T., Cetina, M., Oručević, F. & Vuletić, V. Observation of cold collisions between trapped atoms and trapped atoms. *Phys. Rev. Lett.* **102,** 223201 (2009).
9. Zipkes, C., Palzer, S., Sias, C. & Köhl, M. A trapped single ion inside a Bose–Einstein condensate. *Nature* **464,** 388–391 (2010).
10. Porras, D. & Cirac, J. I. Effective quantum spin systems with trapped ions. *Phys. Rev. Lett.* **92,** 207901 (2004).
11. Friedenauer, A., Schmitz, H., Glueckert, J. T., Porras, D. & Schaetz, T. Simulating a quantum magnet with trapped ions. *Nature Phys.* **4,** 757–761 (2008).
12. Schmied, R., Wesenberg, J. H. & Leibfried, D. Optimal surface-electrode trap lattices for quantum simulation with trapped ions. *Phys. Rev. Lett.* **102,** 233002 (2009).
13. Micheli, A., Brennen, G. K. & Zoller, P. A toolbox for lattice-spin models with polar molecules. *Nature Phys.* **2,** 341–347 (2006).
14. Volz, T. *et al.* Preparation of a quantum state with one molecule at each site of an optical lattice. *Nature Phys.* **2,** 692–695 (2006).
15. Ni, K.-K. *et al.* A high phase-space-density gas of polar molecules. *Science* **322,** 231–235 (2008).
16. Wineland, D. J. *et al.* Experimental issues in coherent quantum-state manipulation of trapped atomic ions. *J. Res. Natl. Inst. Stand. Technol.* **103,** 259–328 (1998).
17. Leibfried, D., Blatt, R., Monroe, C. & Wineland, D. Quantum dynamics of single trapped ions. *Rev. Mod. Phys.* **75,** 281–324 (2003).
18. Schaetz, T., Friedenauer, A., Schmitz, H., Petersen, L. & Kahra, S. Towards (scalable) quantum simulations in ion traps. *J. Mod. Opt.* **54,** 2317–2325 (2007).
19. Drakoudis, A., Söllner, M. & Werth, G. Instabilities of ion motion in a linear Paul trap. *Int. J. Mass Spectrom.* **252,** 61–68 (2006).
20. Friedenauer, A. *et al.* High power all solid state laser system near 280 nm. *Appl. Phys. B* **84,** 371–373 (2006).
21. Grimm, R., Weidemüller, M. & Ovchinnikov, Y. B. Optical dipole traps for neutral atoms. *Adv. Atom. Mol. Opt. Phys.* **42,** 95–170 (2000).
22. Tuchendler, C., Lance, A. M., Browaeys, A., Sortais, Y. R. P. & Grangier, P. Energy distribution and cooling of a single atom in an optical tweezer. *Phys. Rev. A* **78,** 033425 (2008).
23. Gordon, J. P. & Ashkin, A. Motion of atoms in a radiation trap. *Phys. Rev. A* **21,** 1606–1617 (1980).
24. Feng, Y., Taylor, L. R. & Calia, D. B. 25 W Raman-fiber-amplifier-based 589 nm laser for laser guide star. *Opt. Express* **17,** 19021–19026 (2009).
25. Leibrandt, D. R., Labaziewicz, J., Vuletić, V. & Chuang, I. L. Cavity sideband cooling of a single trapped ion. *Phys. Rev. Lett.* **103,** 103001 (2009).
26. Cirac, J. I. & Zoller, P. A scalable quantum computer with ions in an array of microtraps. *Nature* **404,** 579–581 (2000).
27. Schmied, R., Roscilde, T., Murg, V., Porras, D. & Cirac, J. I. Quantum phases of trapped ions in an optical lattice. *New J. Phys.* **10,** 045017 (2008).
28. Kollath, C., Köhl, M. & Giamarchi, T. Scanning tunneling microscopy for ultracold atoms. *Phys. Rev. A* **76,** 063602 (2007).
29. Gehm, M. E., O'Hara, K. M., Savard, T. A. & Thomas, J. E. Dynamics of noise-induced heating in atom traps. *Phys. Rev. A* **58,** 3914–3921 (1998).

Additional information

The authors declare no competing financial interests. Supplementary information accompanies this paper at www.nature.com/naturephotonics. Reprints and permission information is available online at http://npg.nature.com/reprintsandpermissions/. Correspondence and requests for materials should be addressed to T.S.